

LETTER Special Section of Papers Selected from ITC-CSCC '96

# A Clock-Feedthrough Compensated Switched-Current Memory Cell

Hyeong-Woo CHA<sup>†</sup>, Satomi OGAWA<sup>†</sup>, and Kenzo WATANABE<sup>†</sup>, Members

**SUMMARY** A clock-feedthrough (CFT) compensation technique using a dummy cell is valid when the CFT current from a switched-current (SI) memory cell is signal-independent. Based on this idea, a SI dummy cell appropriate for the S<sup>2</sup>I cell is developed. Simulations show that the CFT rejection ratio as high as 60 dB is attainable over the temperature range from  $-30^{\circ}\text{C}$  to  $80^{\circ}\text{C}$  with this architecture. The CFT-compensated SI cell proposed here is, therefore, quite useful for high-accuracy, current-mode signal processing.

**key words:** current-mode signal processing, S<sup>2</sup>I memory cell, clock-feedthrough compensation

## 1. Introduction

A switched-current (SI) cell is an op-amp equivalent in current-mode, sampled-analog signal processing [1], [2]. The performance of the second-generation SI cell as a building block can be measured in terms of the input/output conductance ratio and the error current due to clock-feedthrough (CFT) [3]. The design technique to realize the high conductance ratio has been established by the regulated cascode configuration, and thus reducing the CFT error is now essential for high-accuracy signal processing.

The CFT error in a SI cell originates from those portions of the control signal and the channel charge of a switch transistor which charge the gate-to-source capacitor  $C_{GS}$  of a memory transistor. The resultant shift in the gate-source voltage produces the erroneous drain current referred to as the CFT current. This voltage-to-current conversion is nonlinear when a memory transistor operates in the saturation region, which makes the CFT current highly dependent on the input signal and invalidates the CFT compensation methods proposed for switched-capacitor circuits [4].

To eliminate the signal-dependence is the most crucial for substantial rejection of the CFT current, because the signal-independent component can be cancelled by the dummy cell method [5], [6]. Such first-generation SI cells have already been developed [7], [8]. This paper describes a CFT-compensated second-generation SI cell designed based on the above idea. The basic block is the S<sup>2</sup>I cell [9]. A dummy stage appropriate for the S<sup>2</sup>I cell is combined to substantially reduce the CFT error.

The operation and the performance estimates will be described in the followings.

## 2. CFT-Compensated S<sup>2</sup>I Cell

Figure 1 (a) shows a basic SI cell and the principles of CFT cancellation. The basic cell samples the input signal current  $i_{in}$  in the sample phase when  $\phi_s = "1,"$  holds it during  $\phi_s = "0,"$  and delivers it to the load when  $\phi_h = "1."$  The current  $i_M$  delivered to the load includes the error component  $\delta_M$  which is caused by the CFT charge stored into  $C_{GS}$  of a memory transistor  $M_1$ . If  $\delta_M$  is signal-independent and can be regarded as the offset current, it can be cancelled by providing the dummy cell whose output current  $\delta_C$  counterbalances  $\delta_M$ . A typical configuration of the dummy cell is shown in Fig. 1 (b).

A CFT-compensated SI cell designed based on the above-mentioned principles of CFT cancellation is shown in Fig. 2 (a). Here,  $M_1$  and  $M_6$  form the coarse stage, and  $M_2$  and  $M_5$  form the fine 1 stage of the S<sup>2</sup>I cell with the cascode configuration.  $M_3$  and  $M_4$  form the fine 2 stage which functions as the dummy cell mirrored with the fine 1 stage. The fine 2 stage takes the same configuration as that of the fine 1 stage so that its output current  $i_2$  cancels the CFT current from the fine 1 stage over the wide temperature range. The cascode current mirror  $M_7$ – $M_{10}$  is provided for polarity inversion of  $i_2$ . All the stages and the current mirror are assumed operating in the saturation region.  $S_1, S_4, S_6,$  and  $S_7$  are nMOS switches, while  $S_2, S_3,$  and  $S_5$  are pMOS switches. These switches are controlled by clock signals whose timing is shown in Fig. 2 (b).

The operation of each stage is as follows:

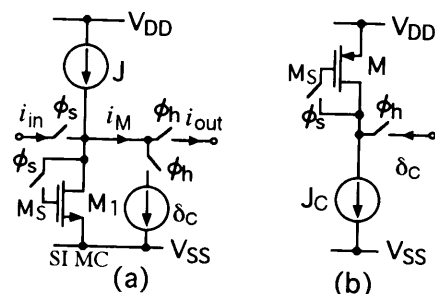


**Fig. 1** A schematic diagram of a CFT-compensated SI cell (a) and a dummy-cell configuration (b).

Manuscript received September 26, 1996.

Manuscript revised January 16, 1997.

<sup>†</sup>The authors are with the Research Institute of Electronics, Shizuoka University, Hamamatsu-shi, 432 Japan.

(i)  $\phi_1 = \phi_{1a} = "1"$  phase: The coarse stage samples  $i_{in}$ . Mirrored with the fine 2 stage, the fine 1 stage operates as current source to provide the bias current  $J_1$  to the coarse stage. The fine 2 stage operates as the load of the current source  $J_1$ . The drain current of each stage is thus given by

$$i_{D1} = J_1 + i_{in}, \quad i_{D2} = J_1, \quad i_{D3} = J_1 \quad (1)$$

(ii)  $\phi_1 = \phi_{1b} = "1"$  phase: Since  $S_1$  is turned off, the coarse stage generates the CFT current  $\delta_1$ .  $S_4$  is still "on" to keep  $i_{in}$  flowing through the coarse stage. The fine 1 stage is now isolated from the fine 2 stage because  $S_5$  is "off," and operates as the load of the coarse stage since  $S_2$  is turned on. The fine 2 stage keeps the operation in the preceding phase. The current of each stage is therefore

$$i_{D1} = J_1 + i_{in} - \delta_1, \quad i_{D2} = J_1 - \delta_1, \quad i_{D3} = J_1 \quad (2)$$

(iii)  $\phi_2 = "1"$  phase: The coarse stage is now isolated from the signal source and operates as the sink current source. Since  $S_2$  and  $S_3$  are turned off, the fine 1 and fine 2 stages generate the CFT current  $\delta_2$  and  $\delta_3$ , respectively. The current flowing each stage is then given by

$$\begin{aligned} i_{D1} &= J_1 + i_{in} - \delta_1, & i_{D2} &= J_1 - \delta_1 + \delta_2, \\ i_{D3} &= J_1 + \delta_3, & \text{and } i_2 &= \delta_3. \end{aligned} \quad (3)$$

The current mirror stage consisting of  $M_7$  and  $M_{10}$  delivers the polarity-inverted  $i_2$  to the output terminal. The output current  $i_{out}$  is therefore

$$i_{out} = i_{D2} - i_{D1} - i_2 = -i_{in} + \delta_2 - \delta_3. \quad (4)$$

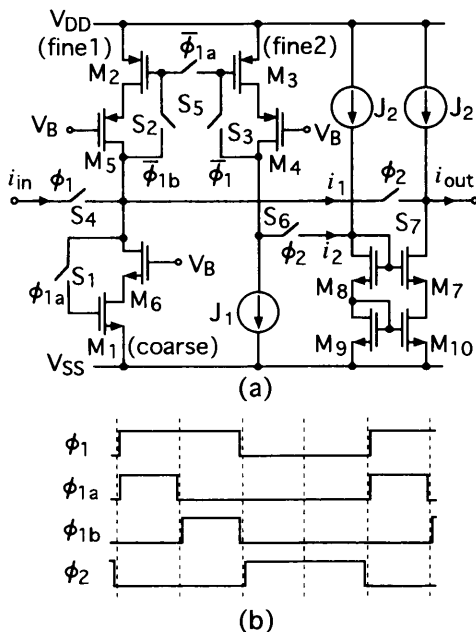


**Fig. 2** The circuit diagram of the CFT-compensated SI cell (a) and timing diagram of clock signals (b).

It should be noted that the signal-dependent CFT  $\delta_1$  does not appear at the output.  $\delta_2$  is given by

$$\delta_2 = \sqrt{2\beta_2 i_{D2}} \left( \frac{Q_{f2}}{C_{GS2}} \right) - \frac{\beta_2}{2} \left( \frac{Q_{f2}}{C_{GS2}} \right)^2, \quad (5)$$

where  $i_{D2} = J_1 - \delta_1$ ,  $\beta_2$  is the gain factor of  $M_2$ , and  $Q_{f2}$  is the CFT charge stored in  $C_{GS2}$ .  $\delta_3$  is also given by (5) with the subscript 2 replaced by 3. Since  $J_1 \gg \delta_1$ ,  $\delta_2$  is hardly dependent on the input signal. Therefore, using matched transistors for the fine 1 and 2 stages, one can substantially reduce the CFT error with this architecture.

### 3. Performance Estimates

The performance of above-described CFT-compensated SI cell have been simulated using SABER [10], with level-2 MOS transistor model for a  $1.2\mu\text{m}$  standard CMOS process. The aspect ratio of each transistor is listed in Table 1. Supply and bias voltages are:  $V_{DD} = 5\text{V}$ ,  $V_{SS} = 0\text{V}$ , and  $V_B = V_{DD}/2$ . The current sources  $J_1$  and  $J_2$  are composed of the cascode current mirrors, and their values are set to  $200\mu\text{A}$  and  $50\mu\text{A}$ , respectively. The frequency of clock  $\phi_1$  is 2 MHz.

Figure 3 shows waveforms observed in the CFT-compensated cell when the input signal current is  $180\mu\text{A}$ . It can be seen that the current  $i_{D1}$  flowing through the coarse stage is  $J_1 + i_{in} = 380\mu\text{A}$  in the  $\phi_1 = \phi_{1a} = "1"$  phase and decreases by the CFT current in the subsequent phase. In the  $\phi_2$  phase, the coarse and fine 1 stages deliver  $i_1 = i_{in} + \delta_2 = 182.26\mu\text{A}$ , and the fine 2 stage delivers  $\delta_3 = 2.26\mu\text{A}$  which counterbalances the CFT component  $\delta_2 = 2.26\mu\text{A}$  in  $i_1$ . The resultant output  $i_{out}$  is the exact replica of  $i_{in}$ . This observation confirms the operation described in the previous section.

Figure 4 shows the CFT current  $\delta_2$  from the fine 1 stage and the residual error  $\Delta\delta = \delta_2 - \delta_3$  as a function of the input signal current. Figure 5 shows their temperature dependence when  $i_{in} = 40\mu\text{A}$ . Due mainly to the variation in the threshold voltage,  $\delta_2$  increases with temperature with the coefficient of  $4,400\text{ppm}/^\circ\text{C}$ . The fine 2 stage also has the same temperature dependence, because of the identical configuration, to reduce the temperature coefficient of  $\Delta\delta$  to  $2\text{ppm}/^\circ\text{C}$  over the

**Table 1** Transistor dimensions used for simulation.

Transistor	W( $\mu\text{m}$ )	L( $\mu\text{m}$ )
M1	36	4.8
M2	64	4.8
M3	64	4.9
M4, M5	60	1.2
M6	20	1.2
M9, M10	100	10
M7, M8	30	2
S1 ~ S3, S5	1.2	1.2
S4, S6, S7	12	1.2

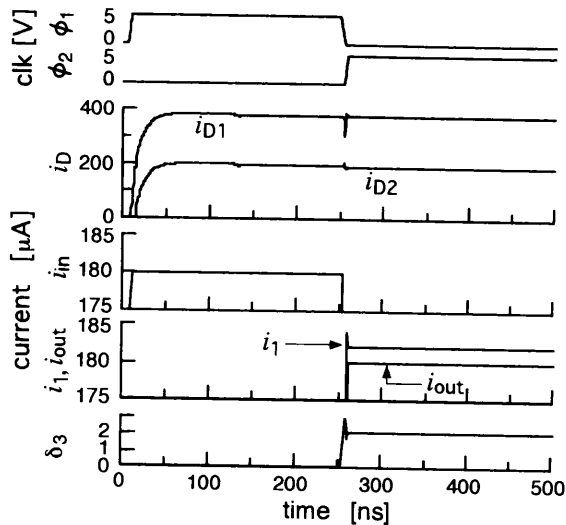


Fig. 3 Current waveforms observed in the CFT-compensated SI cell.

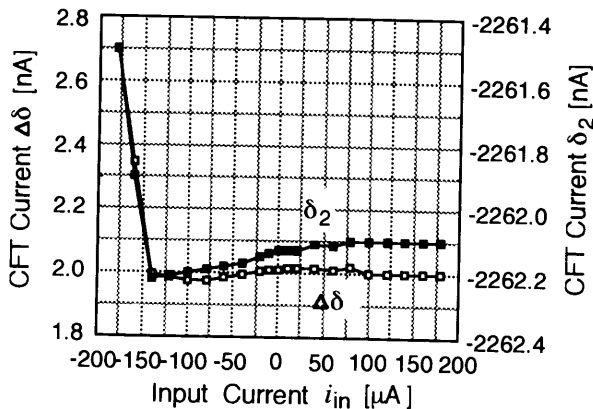


Fig. 4 CFT currents as a function of the input signal current.

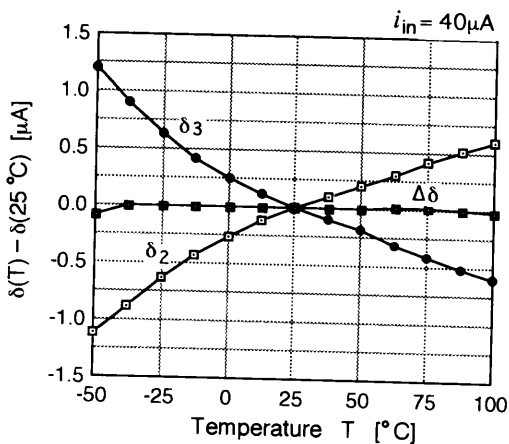


Fig. 5 Temperature dependence of CFT currents.

current mirror also degrade the CFT rejection capability. Their effects are also simulated using typical values [11]. Simulations show that 1% mismatch between  $S_2$  and  $S_3$ , which is an optimistic value for a recent process, degrades the CFT rejection to 40 dB, while each 0.2% mismatch in the current mirror and in the current sources  $J_2$  [2], which is typical for the transistor dimensions quoted in Table 1, to 50 dB. It follows therefore that the careful arrangement of the fine 1 and 2 stages is essential for the high CFT rejection.

4. Conclusions

A CFT-compensated second-generation SI cell using a dummy cell was described. Simulations have shown that the high CFT rejection is possible with this architecture over the wide dynamic and temperature ranges. The performance is amenable to transistor mismatches, however, and a careful layout is essential for substantial reduction of CFT errors. The cell has just been fabricated using a 0.6 μm CMOS process. Its performances will be reported elsewhere.

References

- [1] J.B. Hughes, N.C. Bird, and I.C. Macbeth, "Switched current-A new technique for analogue sampled-data signal processing," Proc. IEEE Int. Symp. Circuits Syst., pp.1584-1587, May 1989,
- [2] C. Toumazou, J.B. Hughes, and N.C. Battersby, "Switched-Currents: an analogue technique for digital technology," chaps. 4 and 6, Peter Peregrinus, London, 1993.
- [3] C. Toumazou, F.J. Lidgley, and D.G. Haigh, "Analogue IC design: the current-mode approach," chap. 11, Peter Peregrinus, London, 1990.
- [4] K. Watanabe and S. Ogawa, "Clock-feedthrough compensated sample/hold circuits," Electronics Letters, vol.24, no.19, pp.1226-1228, Sept. 1988.
- [5] H.C. Yang, T.S. Fiez, and D.J. Allstot, "Current-feedthrough effects and cancellation techniques in switched-current circuits," Proc. Int. Symp. Circuits and Systems, pp.3186-3188, 1990
- [6] Z. Wang, "Current-mode CMOS integrated circuits for analog computation and signal processing: A tutorial," Analog Integrated Circuits and Signal Processing 1, pp.287-295, 1991.
- [7] M. Song, Y. Lee, and W. Kim, "A clock feedthrough reduction circuit for switched-current systems," IEEE J. Solid-State Circuits, vol.28, no.2, pp.133-137, Feb. 1993.
- [8] H-W. Cha and K. Watanabe, "A clock-feedthrough and offset compensated fully-differential switched-current circuit," IEICE Trans. Fundamentals, vol.E78-A, no.11, pp.1531-1533, Nov. 1995.
- [9] J.B. Hughes and K.W. Moulding, "S<sup>2</sup>I: A switched-current technique for high performance," Electronics Letters, vol.29, no.16, pp.1400-1401, Aug. 1993.
- [10] Electronics Staff, "SABER cuts SPICE out of analog simulation," Electronics Magazine, vol.59, no.2, pp.80-92, 1987.
- [11] R.L. Geiger, P.E. Allen, and N.R. Strader, "VLSI design techniques for analog and digital circuits," chap.2, McGraw-Hill, 1990.

range from -30°C to 80°C. These results indicate that the CFT rejection ratio, defined as  $\delta_2/\Delta\delta$ , as high as 60 dB is achievable with the proposed SI cell over the wide dynamic and temperature ranges.

The above simulations assume 2% mismatch between  $M_2$  and  $M_3$ , as can be seen in Table 1. The mismatch between  $S_2$  and  $S_3$  and the gain error of the